Sphingolipid bases. A revisitation of the *O*-methyl derivatives of sphingosine. Isolation and characterization of diacetate derivatives, with revised ^{13}C nuclear magnetic resonance assignments for D-*erythro*-sphingosine

Alemka Kisic, Mitsuhiro Tsuda,[1] Richard J. Kulmacz,[2] William K. Wilson, and George J. Schroepfer, Jr.[3]

Departments of Biochemistry and Cell Biology and of Chemistry, Rice University, P.O. Box 1892, Houston, TX 77251

Abstract As described by Carter et al. (*J. Biol. Chem.* 1951. **192:** 197–207), *O*-methyl derivatives of sphingosine are formed upon acid hydrolysis of sphingolipids in the presence of methanol. In the present study, we have isolated four *O*-methyl ethers of C_{18}-sphingosine by medium pressure liquid chromatography of their diacetate derivatives, i.e., (2S,3R,4E)-1-acetoxy-2-acetamido-3-methoxy-4-octadecene, its (2S,3S) epimer, (2R,3E,5R)-1-acetoxy-2-acetamido-5-methoxy-3-octadecene, and its (2R,5S) epimer. Structures were determined by physical, chromatographic, and spectral properties. The 5-*O*-methyl ethers, which were the predominant byproducts of sphingolipid hydrolysis, were easily distinguished from the 3-*O*-methyl ethers by chromatography, and all four isomers could be differentiated by ^{1}H and ^{13}C nuclear magnetic resonance (NMR) spectroscopy. NMR analysis of the original *N*-acetate and diacetate samples of *O*-methylsphingosines I and II of Carter et al. demonstrated that they correspond to the 5-*O*-methyl ethers (2R,5R and 2R,5S, respectively), with purities of ~90–99%. Resolution enhancement of the 126-MHz ^{13}C NMR spectra of the *O*-methyl ethers and D-*erythro*-C_{18}-sphingosine (**Ia**) afforded distinct signals for nearly all carbon atoms. ^{13}C NMR assignments of carbons 7–15 were made from their lanthanide-induced shifts, and revised assignments for olefinic carbons of **Ia** were established based upon ^{1}H-^{13}C shift correlation experiments. **—Kisic, A., M. Tsuda, R. J. Kulmacz, W. K. Wilson, and G. J. Schroepfer, Jr.** Sphingolipid bases. A revisitation of the *O*-methyl derivatives of sphingosine. Isolation and characterization of diacetate derivatives, with revised ^{13}C nuclear magnetic resonance assignments for D-*erythro*-sphingosine. *J. Lipid Res.* 1995. **36:** 787–803.

Supplementary key words medium pressure liquid chromatography • lanthanide-induced shifts

Sphingolipids are an important class of compounds that are essentially unique to eukaryotes. Long-chain sphingolipid bases represent the defining elements of sphingolipids. The bulk of the sphingolipid bases in cells occurs in the form of more complex entities such as sphingomyelins, gangliosides, and other glycosphingolipids. These complex sphingolipids have been shown to be important antigens in both normal and tumor cells (1), and certain complex sphingolipids have been implicated in receptor functions for toxins, hormones, viruses, and other ligands (2–4) and may play roles in differentiation and oncogenic transformation (5, 6). The importance of these complex sphingolipids is further indicated by the occurrence of human disease entities involving inherited defects in their intermediary metabolism (7, 8). In addition, a requirement of sphingolipids for normal cell replication has been demonstrated in a temperature-sensitive mutant of Chinese hamster ovary cells (CHO-K1) defective in serine palmitoyltransferase (9). Apart from their involvement as components of complex sphingolipids, additional functions for sphingolipid bases in cellular physiology have been suggested. Considerable attention has recently been directed towards free sphingolipid bases and

Abbreviations: COSY, ^{1}H-^{1}H correlation spectroscopy; COSYDEC, f_1-decoupled COSY; GC, gas chromatography; HMBC, heteronuclear multiple bond correlation; HPLC, high performance liquid chromatography; HSQC, ^{1}H-^{13}C heteronuclear single quantum coherence; IR, infrared (spectrum); LIS, lanthanide-induced shift; mp, melting point; MPLC, medium pressure liquid chromatography; MS, mass spectrometry or mass spectrum; NMR, nuclear magnetic resonance; $Pr(tfc)_3$, tris[3-(trifluoromethylhydroxymethylene)-(+)-camphorato]praseodymium(III); TLC, thin-layer chromatography; TMS, trimethylsilyl.

[1]Present address: National Institute of Health Sciences, Tokyo, Japan.

[2]Present address: Department of Medicine, University of Texas Health Science Center at Houston, Houston, Texas.

[3]To whom inquiries should be directed.

their 1-phosphate and *N*-acyl derivatives as potential regulators of a variety of cellular processes (10–14). Pursuit of these matters requires the availability of sphingolipid bases (and their derivatives) of known structure and purity.

D-*Erythro*-C_{18}-sphingosine (**Ia**) is a major sphingolipid base in most animal tissues. Brain and spinal cord represent particularly rich sources of sphingolipids from which enantiomerically pure **Ia** can be prepared in quantity (15). However, hydrolysis of sphingolipids results in the formation of byproducts that complicate analyses of sphingolipid base composition and present problems in the isolation of pure D-*erythro*-sphingosine from natural sources (16–18). *O*-Methyl ethers have long been recognized as one type of byproduct formed during acid hydrolysis of sphingolipids in the presence of methanol (16, 19). In the present study we describe the first isolation of each epimer of the 3-*O*-methyl and 5-*O*-methyl derivatives of C_{18}-sphingosine by medium pressure liquid chromatography (MPLC) of their diacetates. Each of the four isomers has been characterized by chromatographic and ^1H and ^{13}C nuclear magnetic resonance (NMR) spectral techniques. Also presented are revised ^{13}C NMR assignments for the olefinic carbons of D-*erythro*-C_{18}-sphingosine (**Ia**); a preliminary account of this latter finding has been presented previously (20). Structures of **Ia** and its *O*-methyl derivatives are shown in **Fig. 1.**

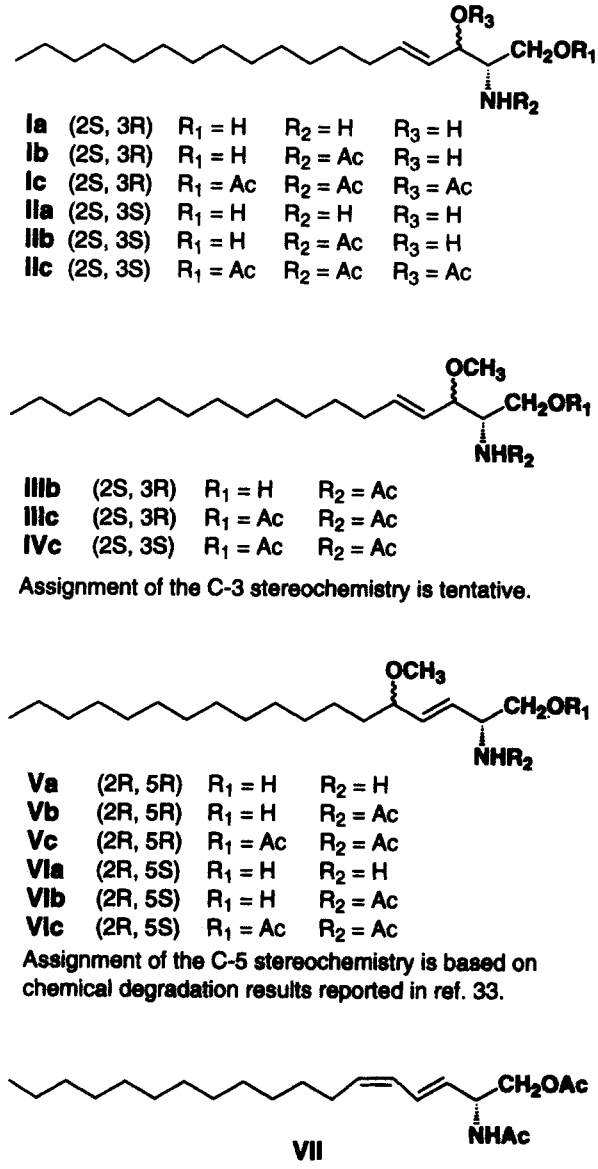

Fig. 1. Structures of D-*erythro*-C_{18} sphingosines (**I**), L-*threo*-C_{18}-sphingosines (**II**), 3-*O*-methyl ethers **III–IV**, 5-*O*-methyl ethers **V-VI**, and diene **VII**.

EXPERIMENTAL PROCEDURES AND RESULTS

Materials and methods

Melting points (mp) were measured with a Thomas-Hoover apparatus. Infrared (IR) spectra were obtained on a Beckman IR-9 spectrometer using KBr pellets. Optical rotations were measured on a JASCO DIP-4 digital polarimeter. Thin-layer chromatography (TLC) was carried out on silica gel G plates (Analtech; Newark, DE) or, for data in **Table 1** only, on aluminum-backed silica gel 60 plates (E. Merck; Gibbstown, NJ). Components on the plates were visualized after spraying with molybdic acid followed by heating. Solvent systems for TLC were: SS-1, chloroform; SS-2, chloroform–methanol 98:2; SS-3, chloroform–methanol 95:5; SS-4, chloroform–methanol 80:20; SS-5, chloroform–methanol–NH_4OH (2 N) 80:20:2. MPLC was done at ~1.5 atm using a single-piston pump, Altex glass columns dry-packed with silica gel (32–63 μm), and a four-way injection valve. High performance liquid chromatography (HPLC) was carried out at 1 ml per min using a 5-μm Customsil ODS reversed phase column (250 mm × 4.6 mm; Custom LC, Houston, TX) and a Waters model 490 UV detector set at 210 nm. Gas chromatography (GC) was carried out isothermally on a Hewlett-Packard model 402 or 5710A instrument with helium (60 ml/min) as the carrier gas, flame-ionization detection, and a glass column (1.8 m × 4 mm i.d.) packed with either 3% OV-1 (methyl polysiloxane) or 3% OV-17 (50% phenyl–50% methyl polysiloxane) on Gas Chrom Q (100–120 mesh). Injector and detector temperatures were set ~25°C above the column temperature. Mass spectra (MS) were recorded on an LKB-9000S (GC–MS) or a ZAB-HF (direct probe) instrument at an electron energy of 70 eV and are reported as *m/z* (% intensity relative to the base peak).

Nuclear magnetic resonance (NMR) spectra were measured on a Bruker AMX500 spectrometer (500.1 MHz for ^1H, 125.8 MHz for ^{13}C) and referenced to

TABLE 1. Properties of D-*erythro*-sphingosine and its 3-*O* methyl and 5-*O* methyl derivatives[a,b]

Compound	mp (°C)	$[\alpha]_D$ (°)	TLC (R_f)	HPLC (t_R, min)	GC (t_R, min)
Diacetate or triacetate					
Ic	104–105	−15.0	0.59	12.0	
IIc	43	+8.4[d]	0.62	12.0	
IIIc 3-*O*-Me	74–75	−12.1	~0.65[†]	14.3	10.1
IVc 3-*O*-Me	52–53.5		0.66	14.9	9.6
Vc 5-*O*-Me	68–69	+6.9			12.4
	68–69[e]	+5.3[e]	0.49[e]	11.5[e]	
VIc, 5-*O*-Me	76–76.5	−10.3			12.4
	74–75[f]	−11.7[f]	0.47[f]	11.8[f]	
VII, diene			~0.60[†]	13.0	
N-Acetate					
Ib	85[g]	−11.2	0.50	8.4	
IIb[h]	73–75	−8.6	0.50	8.8	
Vb, 5-*O*-Me	73–74				
	75–76[e]	−2.5[e]	0.53[e]	9.5[e,i]	
VIb, 5-*O*-Me	77–78.5				
	77–78[f]	−21.4[f]	0.53[f]	9.7[f,i]	
Free base					
Ia	84–86[j]	−1[k]	0.20		
IIa	86.5–87.5	−1	0.19		
Va, 5-*O*-Me	64–65[e]	+11.4[e]	~0.29[†]		
VIa, 5-*O*-Me	87–88[f]	−15.7[f]	0.29[f]		

[a]Conditions for HPLC (water–methanol 10:90) and GC (OV-17; 240°C) are given in the Experimental section. Optical rotations were measured in chloroform (*c* 1.4 for **Ia** and *c* 0.3 for **IIb** and **IIc**). The TLC solvents were SS-3 (diacetates and triacetates), SS-4 (*N*-acetates), and SS-5 (free bases).

[b]Approximate R_f values based on TLC of mixtures are indicated by †.

[c]Additional recent physical constants for **Ia, IIa, Ic,** and **IIc** of synthetic origin are given in ref. 27 and 30 and references cited therein.

[d]Data from ref. 26.

[e]Data for the corresponding derivative of *O*-methylsphingosine I (mp and $[\alpha]_D$ from ref. 19).

[f]Data for the corresponding derivative of *O*-methylsphingosine II (mp and $[\alpha]_D$ from ref. 19).

[g]See footnote 7 of text.

[h]Sample of 90–95% purity.

[i]The N-acetyl derivatives of the 5-*O*-methyl ethers were partially resolved by HPLC in water–methanol 15:85: t_R 15.0 min (**Ib**), 17.7 min (**Vb**), 18.1 min (**VIb**).

[j]Data from ref. 23.

[k]The rotation in methanol is +10.9° (ref. 23).

internal tetramethylsilane (^1H) or $CDCl_3$ at 77.0 ppm (^{13}C). Unless otherwise indicated, spectra were recorded at 25°C at a sphingolipid concentration of ~60 mM (^{13}C) or ~5 mM (^1H). Some 1D spectra were resolution-enhanced by Gaussian apodization, i.e., multiplication of the free induction decay spectrum by the function $\exp(-\pi LB(t - \frac{t^2}{2GB \cdot AQ}))$, where AQ is the acquisition time and typically LB = −2 and GB = 0.4. Standard Bruker software was used to acquire double-quantum filtered COSY (^1H-^1H correlation spectroscopy) and COSYDEC (f_1-decoupled COSY, 0.2-s fixed evolution period τ_e) spectra, both acquired with 256 t_1 increments spanning a spectral window of δ −0.2 to 7.6. HMBC (heteronuclear multiple bond correlation) spectra, with ~100 t_1 increments, f_2 δ −0.2 to 7.6, and f_1 typically δ 160–179, were used to assign acetate ^1H and ^{13}C signals. HSQC (^1H-^{13}C heteronuclear single quantum coherence) spectra (21) were acquired using ^{13}C decoupling with either a full spectral window in f_1 (typically ~200 t_1 increments) or with an f_1 window encompassing only the olefinic ^{13}C signals (parameters given in the legend of **Fig. 2**); the f_2 window in all 2D spectra was δ −0.2 to 7.6. COSY and HSQC spectra were acquired in a phase-sensitive mode (time-proportional phase increments and States, respectively). Coupling constants were calculated by averaging all appropriate line spacings in resolution-enhanced spectra. Sample purities were generally estimated by summing the levels of each minor contaminant observed in the ^1H NMR spectrum (δ 1.9–6.7 region; little or no resolution enhancement; detection limit typically ≤1%). All NMR data in the Tables are from the AMX500 instrument; additionally, ^{13}C spectra of **IIIb, IIIc, IVc, Vc,** and

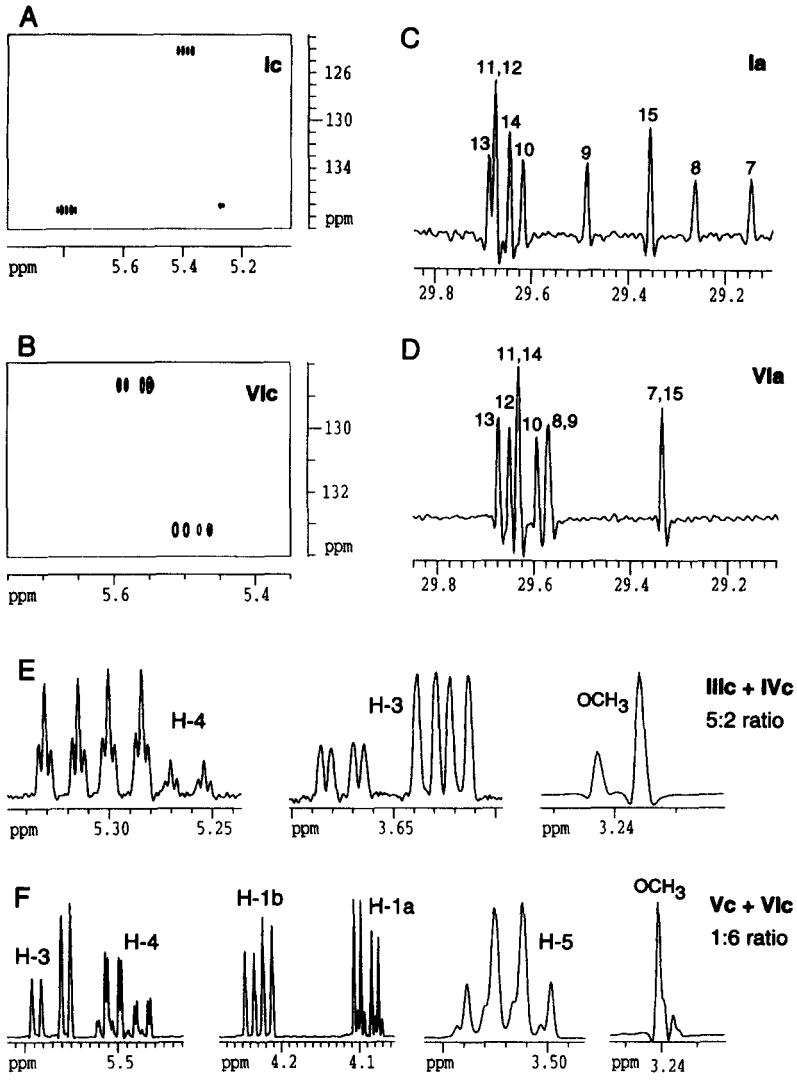

Fig. 2. NMR spectra of sphingolipid bases. Panel A, HSQC spectrum of the olefinic region of **Ic** (δ_H −0.2 to 7.6 in f_2; δ_C 120–141 in f_1, 48 t_1 increments of 32 scans each, delays optimized for $^1J_{CH}$ of 147 Hz, ^{13}C decoupling). Panel B, HSQC spectrum of olefinic region of **VIc** (δ_C 126–137 in f_1, 42 t_1 increments of 32 scans each, other parameters as in panel A). Panel C, portion of the 126-MHz ^1H-decoupled ^{13}C NMR spectrum of **Ia** (Gaussian apodization, 128k points, 1-s acquisition time). Panel D, portion of the 126-MHz ^1H-decoupled ^{13}C NMR spectrum of **VIa** (conditions as in panel C). Panel E, portions of the 500-MHz ^1H NMR spectrum of a 5:2:8 mixture of **IIIc, IVc,** and **VII** (~5 mM in $CDCl_3$; fractions 33–44 from column F) showing partial resolution of signals for **IIIc** and **IVc** (signals of **VII** are outside spectral regions shown). Panel F, portions of the 500-MHz ^1H NMR spectrum of a 1:6 mixture of **Vc** and **VIc** (~60 mM in $CDCl_3$). Spectral parameters for E and F: 2.7-s acquisition time, 32k points, mild Gaussian apodization; 0.01 ppm spacing of tick marks. The poor peak shape for the methoxy resonance in panel F is representative of shimming problems often encountered at higher concentrations (~60 mM) of sphingolipid bases.

VIc isolated by MPLC were acquired at 25 MHz on a Varian XL-100 spectrometer.[4]

Lanthanide-induced shifts (LIS) for **Ia** were determined by adding 2–160 μl of a 114 mM solution of tris[3-(trifluoromethylhydroxymethylene)-(+)-camphorato]praseodymium(III) ($Pr(tfc)_3$) in $CDCl_3$ to a 79 mM solution of **Ia** in $CDCl_3$. ^{13}C NMR spectra were collected at 25°C for eight molar ratios (0.005 to 0.487) of $Pr(tfc)_3$ to **Ia.** Data for carbons 1–3 were unavailable at higher molar ratios owing to severe line broadening. No corrections were

[4]Samples of **IIIc, IVc, Vc,** and **VIc** isolated by MPLC and two *N*-acetate derivatives were originally characterized by ^{13}C NMR at 25 MHz (XL-100 instrument) at high concentration (>0.1 M). Except for 1 mg each of **IIIc** and **Vc,** these samples were not available for high-field NMR studies, and spectra of **Vb, Vc, VIa, VIb,** and **VIc** were measured on authentic samples obtained from H. E. Carter (19). After compensation for concentration and temperature differences, the 126-MHz ^{13}C NMR spectra of **Vc** and **VIc** were found to correspond to those of the 25-MHz spectra. NMR data for **IIIc** and **IVc** were derived from the ^1H NMR spectrum of **IIIc** and spectra of mixtures of **IIIc, IVc,** and **VII** (fractions 29–32 and fractions 33–44 from column F). Portions of the latter spectrum are shown in Fig. 2, panel E.

TABLE 2. ^{13}C NMR chemical shifts for D-*erythro*- and L-*threo*-sphingosines **I–II**, 3-*O*-methyl ethers **III–IV**, 5-*O*-methyl ethers **V–VI**, and diene **VII**[a–c]

	D-*erythro*- and L-*threo*-Sphingosines						3-*O*-methyl		5-*O*-methyl					Diene
Conc[d]	**Ia** 79	**IIa** 12	*N*-Ac **Ib** 68	*N*-Ac **IIb** 56	tri-Ac **Ic** 63	tri-Ac **IIc** 56	di-Ac **IIIc** 55	di-Ac **IVc** 72	**VIa** 64	*N*-Ac **Vb** 67	*N*-Ac **VIb** 70	di-Ac **Vc** 60	di-Ac **VIc** 58	di-Ac **VII** 55
C-1	63.73	64.86	62.24	64.15	62.58	63.08	62.75	63.44	66.49	65.43	65.49	65.60	65.71	65.73
C-2	56.17	56.49	54.52	54.80	50.64	50.85	51.80	51.72	54.64	52.83	52.87	49.60	49.57	50.17
C-3	75.10	73.94	74.43	73.00	73.80	73.04	82.39	80.00	133.70	129.01	128.99	128.49	128.56	128.13**
C-4	129.14	129.76	128.66	128.91	124.11	124.05	125.99	125.66	132.03	133.36	133.24	133.42	133.17	128.16**
C-5	134.65	134.29	134.20	134.07	137.41	137.33	137.14	136.68	81.97	81.70	81.75	81.65	81.71	127.14
C-6	32.34	32.31	32.27	32.26	32.26	32.25	32.28	32.28	35.41	35.31	35.27	35.36	35.32	134.05
C-7	29.17	29.13	29.12	29.13	28.87	28.78	29.11	29.11	25.33	25.31	25.27	25.27	25.23	27.84
C-8	29.26	29.21	29.20	29.21	29.14	29.12	29.15	29.15	29.57	29.57	29.55*	29.57	29.55*	29.27*
C-9	29.48	29.47	29.47	29.49	29.43	29.41	29.44	29.44	29.57	29.57	29.57*	29.57	29.56*	29.51*
C-10	29.61	29.60	29.60	29.61	29.57	29.56	29.58	29.58	29.60	29.60	29.60	29.60	29.60	29.55*
C-11	29.67	29.66	29.66	29.68	29.64	29.64	29.64	29.64	29.64	29.63	29.63	29.62*	29.62	29.60*
C-12	29.67	29.66	29.66	29.67	29.64	29.64	29.64	29.64	29.65	29.65	29.65	29.64	29.64	29.64
C-13	29.68	29.68	29.67	29.67	29.66	29.66	29.66	29.66	29.68	29.67	29.67	29.67	29.67	29.66
C-14	29.64	29.64	29.63	29.64	29.63	29.63	29.62	29.62	29.64	29.63	29.63	29.63*	29.62	29.62
C-15	29.34	29.35	29.33	29.34	29.33	29.33	29.33	29.33	29.34	29.33	29.33	29.33	29.33	29.33
C-16	31.91	31.91	31.90	31.91	31.90	31.90	31.90	31.89	31.90	31.90	31.90	31.90	31.90	31.90
C-17	22.67	22.68	22.66	22.67	22.66	22.66	22.66	22.66	22.67	22.66	22.66	22.66	22.66	22.66
C-18	14.10	14.11	14.09	14.10	14.09	14.09	14.09	14.09	14.10	14.09	14.09	14.09	14.09	14.09
1-OAc					20.79	20.75	20.88	20.85				20.76	20.76	20.81
					170.94	170.66	171.10	170.90				170.98	170.98	171.07
2-NAc			23.35	23.32	23.34	23.26	23.42	23.29		23.38	23.36	23.36	23.36	23.39
			170.91	171.28	169.63	169.81	169.63	169.93		170.39	170.47	169.36	169.41	169.40
3-OR'					21.11	21.08	56.54	56.25	56.11	56.28	56.28	56.25	56.18	
					169.96	170.09								

[a]Data obtained at 125 MHz at 25°C and referenced to $CDCl_3$ at 77.0 ppm.
[b]Assignments for entries marked by * or ** may be interchanged within a column.
[c]Data for **IIIc, IVc,** and **VII** extracted from spectra of mixtures of these compounds (1:10:2 and 5:2:8). The ^{13}C NMR spectrum of a 5:1 mixture of **VIa:Va** showed only two resolved signals for **Va:** 54.57 (C-2) and 131.97 (C-4).
[d]Concentration (mM) of sphingolipid base in $CDCl_3$. Total sphingolipid base concentration is given for data obtained from mixtures (**IIIc, IVc,** and **VII**).
[e]R = Ac for **Ic** and **IIc**; R = CH_3 for O-methyl ethers.

made for contact shifts. The relative LIS values were obtained by linear regression calculations (intercept fixed at 0) on the plot of induced shifts versus apparent molar ratio of $Pr(tfc)_3$ to **Ia,** followed by normalization to the LIS of C-2. The apparent molar ratios, which were calculated for seven data sets from weighted ratios of all nonzero ^{13}C-induced shifts relative to those of the 0.024 molar ratio data set, were similar to ratios based on volumetric measurements. LIS for *O*-methylsphingosine II (**VIa**) were determined similarly using 159 mM $Pr(tfc)_3$ and 74 mM **VIa** in $CDCl_3$ (eight molar ratios from 0.011 to 0.610). Extrapolated to a 1:1 molar ratio of $Pr(tfc)_3$ to substrate, the LIS for C-2 was 37 ppm for **Ia** and 38 ppm for **VIa.**[5] The least squares fits were quite good as judged by the average of the residuals (absolute values), which was <0.02 ppm for polarizable carbons (C-1 through C-5 and methoxyl) and <0.005 ppm for other carbons.

TMS ethers for analysis by GC were prepared essentially as described by Carter and Gaver (22). $Pr(tfc)_3$ was obtained from Aldrich Chemical Co. (Milwaukee, WI). Samples of *O*-methylsphingosine II (**VIa**), its *N*-acetate (**VIb**) and diacetate (**VIc**) derivatives, and the *N*-acetate (**Vb**) and diacetate (**Vc**) derivatives of *O*-methylsphingosine I were gifts from H. E. Carter. Despite storage for >40 years under refrigeration, these samples from the original work of Carter, Nalbandov, and Tavormina (19) showed remarkably high purity by NMR analysis: **Vb,** ~99% purity; **Vc,** ~90% purity (contained 5% **Ic** and 3% **VIc**); **VIa,** ~90% purity; **VIb,** ~98% purity; **VIc,** 95% purity (<1% **Vc**).

Preparation of D-*erythro*-C_{18}-sphingosine (Ia), its L-*threo* isomer (IIa), and their acetate derivatives

D-*Erythro*-C_{18}-sphingosine[6] (**Ia**) and its L-*threo* isomer **IIa** were prepared as described previously (20, 23). Tri-

[5]Because the praseodymium shift reagent produced mainly upfield induced shifts, the upfield LIS have been designated as positive numbers.

[6]Chemical Abstracts nomenclature for representative sphingolipid bases described herein: **Ia,** 2-amino-4-octadecene-1,3-diol; **Va,** 2-amino-5-methoxy-3-octadecen-1-ol; **Ic,** *N*-[2-acetyloxy-1-(acetyloxymethyl)-3-heptadecenyl]acetamide; **IIIc,** *N*-[2-methoxy-1-(acetyloxymethyl)-3-heptadecenyl]acetamide; **Vc,** *N*-[4-methoxy-1-(acetyloxymethyl)-2-heptadecenyl]acetamide; **VII,** *N*-[1-(acetyloxymethyl)-2,4-heptadecadienyl]acetamide.

TABLE 3. ^{1}H NMR chemical shifts for D-*erythro*- and L-*threo*-sphingosines **I–II**, 3-*O*-methyl ethers **III–IV**, 5-*O*-methyl ethers **V–VI**, and diene **VII**[a–d]

	D-*erythro*- and L-*threo*-Sphingosines						3-*O*-methyl		5-*O*-methyl						Diene
	Ia	**IIa**	*N*-Ac **Ib**	*N*-Ac **IIb**	tri-Ac **Ic**	tri-Ac **IIc**	di-Ac **IIIc**	di-Ac **IVc**	**Va**[e]	**VIa**	*N*-Ac **Vb**	*N*-Ac **VIb**	di-Ac **Vc**	di-Ac **VIc**	di-Ac **VII**
H-1a	3.627	3.546	3.713	3.816	4.042	4.063	4.141	4.134	3.351	3.352	3.688	3.689	4.087	4.092	4.109
H-1b	3.689	3.682	3.979	3.840	4.304	4.093	4.291	4.143	3.625	3.613	3.743	3.738	4.233	4.235	4.208
H-2	2.888	2.795	3.911	3.921	4.433	4.398	4.25†	4.219	3.45†	3.490	4.596	4.591	4.817	4.815	4.831
H-3	4.056	3.984	4.343	4.388	5.277	5.407	3.625	3.675	5.607	5.606	5.624	5.622	5.565	5.568	5.534
H-4	5.476	5.462	5.542	5.486	5.391	5.380	5.308	5.278	5.494	5.494	5.530	5.527	5.501	5.491	6.510
H-5	5.766	5.750	5.794	5.753	5.792	5.773	5.722	5.701	3.509†	3.510	3.540	3.543	3.524	3.519	5.936
H-6a	2.05†	2.04†	2.05†	2.03†	2.04†	2.02†	2.05†	2.04†		1.44	1.45	1.45	1.42	1.43	5.478
H-6b	2.07†	2.06†	2.07†	2.04†	2.05†	2.03†	2.07†	2.06†		1.58	1.58	1.57	1.57	1.56	
H-7a	1.37†	1.37†	1.37†	1.36†	1.35†	1.34†	1.37†	1.37†		1.28†					2.15†
H-7b	1.37†	1.37†	1.37†	1.36†	1.35†	1.34†	1.37†	1.37†		1.33†					2.17†
H-18	0.881	0.881	0.881	0.880	0.880	0.880	0.880	0.880	0.880	0.880	0.880	0.880	0.880	0.880	0.880
N-H	1.90	1.75	6.28	6.12	5.63	5.63	5.74	5.74	1.72	1.73	5.79	5.77	5.67	5.66	5.64
1-OAc					2.071	2.070	2.049	2.058					2.068	2.066	2.017
2-NAc			2.050	2.042	1.984	2.001	1.983	1.993			2.050	2.051	2.023	2.027	2.075
3-OR[f]					2.064	2.079	3.236	3.243	3.249	3.256	3.254	3.263	3.237	3.242	

[a]Data referenced to internal $(CH_3)_4Si$ from ^{1}H spectra at 500 MHz in $CDCl_3$ solution at 25°C and a concentration of ~5 mM. Chemical shifts for H-8 through H-17 were δ 1.25–1.30 (mainly δ 1.27).

[b]Estimated accuracy ±0.002 ppm (values given to three decimal places) or ±0.01 ppm (values given to two decimal places) except for entries marked by † (±0.02 ppm). However, in a few spectra (especially among the free bases), chemical shifts in the polar head group differed from these values by up to 0.2 ppm, perhaps owing to adventitious contaminants.

[c]No stereochemical assignments are given for protons at C-1, C-6, or C-7. The upfield protons are labeled as a, the downfield protons as b.

[d]Data for **IVc** and **VII** extracted from spectra of mixtures of **IIIc, IVc,** and **VII** (*1:10:2* and *5:2:8*).

[e]Chemical shifts extracted from a ^{1}H difference spectrum obtained by subtracting a spectrum of **VIa** from the spectrum of a 5:1 mixture of **VIa:Va.**

[f]R = Ac for **Ic** and **IIc**; R = CH_3 for *O*-methyl ethers.

acetyl sphingosine (**Ic**) was prepared by treatment of sphingosine (154 mg) with pyridine (1 ml) and acetic anhydride (1 ml) for 2 h at room temperature. Evaporation to dryness followed by recrystallization from hexane–methanol gave **Ic** (139 mg): mp 104–105°C, lit. mp 103.5–104°C (24); $[\alpha]_D^{24}$ −15.0° (*c* 1.0, chloroform); IR, ν_{max} 3300, 3100, 3000–2920, 1740, 1660, 1555, 1470, 1380, 1270, 1240, 1030, 610 cm^{-1}; ^{13}C NMR, **Table 2;** ^{1}H NMR **Table 3;** ^{1}H-^{1}H NMR coupling constants, **Table 4.** *N*-Acetyl sphingosine (**Ib**) was prepared by hydrolysis of **Ic** (135 mg) with 0.1 N KOH in methanol–water 9:1 (15 ml) at room temperature for 20 h. After evaporation of the methanol and addition of water (3 ml), the mixture was extracted with ether (3 × 40 ml). The ether extracts were washed with water until neutral, dried over Na_2SO_4, and evaporated to a residue (97 mg) that was recrystallized from hexane–methanol to give **Ib** (70 mg): mp 85°C,[7] lit. mp 85–87°C (25); $[\alpha]_D^{24}$ −11.2° (*c* 0.6, chloroform), lit. $[\alpha]_D^{26}$ −10.0° (*c* 13.7, methanol) (25); single component by TLC in SS-5 (R_f 0.72) and by GC (OV-1) of the TMS ether at 230°C (t_R 11.8 min); IR, ν_{max} 3300, 3080, 2980–2920, 1655, 1550, 1475, 1380, 1050, 960, 720 cm^{-1}; ^{1}H and ^{13}C NMR, Tables 2–4; 98% purity by ^{1}H NMR. The N-acetate (**IIb**) and triacetate (**IIc**) derivatives of L-*threo*-C_{18}-sphingosine were prepared analogously to **Ib** and **Ic.** Characterization of **IIa, IIb,** and **IIc**[8] is given in Tables 1–4.

Isolation of *O*-methyl-sphingosines as the diacetate derivatives (Fig. 3)

Beef brain sphingolipids (50 g) prepared as described previously (15) were refluxed in a mixture of methanol (800 ml), concentrated HCl (83 ml), and water (117 ml) for 18 h. The cooled mixture was extracted with petroleum ether (2 × 500 ml) to remove fatty acids. The aqueous layer was neutralized with 12 N KOH (120 ml), followed by addition of water (350 ml) and extraction with chloroform (1600 ml). The chloroform extracts were washed with a mixture of chloroform–methanol–water 3:48:47 (1000 ml) and evaporated to a residue (11.48 g). The crude sphingolipid base preparation was subjected to MPLC (1000 mm × 25 mm silica gel column; elution with chloroform–methanol 85:15; column A). As shown in Fig. 3, fractions 41–76 contained *O*-methyl ethers, and later fractions contained **Ia,** its *threo* isomer, and its di-

[7]At 85°C, the crystalline material condensed into several clear blobs, which became a clear mobile liquid at 95°C.

[8]Our melting point for **IIc** (43°C) agrees with values reported in ref. 26 (43–43.5°C) and ref. 27 (42–44°C) and differs markedly from those reported for *dl*-**IIc** by others (28, 29). Our NMR spectral data for **IIc** are similar to those reported in ref. 26, 27, and 30 but differ from those in ref. 28.

hydro derivative (analyses based mainly on TLC and GC). Unidentified nonpolar material (R_f 0.9 in SS-5) was the major component in fractions 1–40 and a minor component in fractions 41–76. The total recovery from column A was 9.4 g (82%). The material from fractions 41–53, 54–58, 59–70, and 71–76 was acetylated and subjected to MPLC (columns B, C, D, and E, respectively), as described below for column C. The results are summarized in Fig. 3.

Compound **IIIc.** Fractions 54–58 from column A were evaporated to a residue (138 mg) that was acetylated overnight at room temperature with pyridine (2 ml) and acetic anhydride (2 ml). The mixture was poured into water and extracted with ether. The ether extracts were washed with 2 N HCl (40 ml) and water and evaporated to a residue (174 mg) that was subjected to MPLC (1000 mm × 9 mm silica gel column; elution with chloroform–methanol 99:1; column C). Evaporation of fractions 14–56 to a residue (54 mg), followed by two recrystallizations from hexane gave **IIIc** (40 mg): mp 74–75°C; single component by TLC in chloroform–methanol 99:1; single component by GC (Table 1); spectral data essentially identical to those given for **IIIc** below (IR and MS) or in Table 2 (^{13}C NMR at 25 MHz). Another sample of **IIIc** (from crystallization of fractions 8–14 of column B) showed ≥95% purity (two unidentified impurities of ~2% by ^{1}H NMR): mp 73.5–74.5°C; $[\alpha]_D^{27}$ −12.1° (*c* 0.4, chloroform); IR, ν_{max} 3300, 3100, 2970–2820, 1740, 1735, 1655, 1550, 1470, 1375, 1260, 1140, 1100, 1040, 965, 725, 630 cm^{-1} (see also **Fig. 4**); MS (ZAB), *m/z* 397 (0.2, M$^+$), 382 (0.3), 365 (4), 338 (33), 281 (20), 278 (7), 267 (8), 262 (6), 253 (100), 170 (12), 144 (25), 123 (9), 109 (13), 102 (22). Additional data for **IIIc** from this sample and from mixtures of **IIIc, IVc,** and **VII** (see below) are presented in Tables 1–4.

Compound **IVc.** Fractions 7–42 from column D were evaporated to an oil (138 mg) that was subjected to MPLC (1000 mm × 9 mm silica gel column; elution with chloroform; column F). Evaporation of fractions 23–28 gave a residue (40 mg) that slowly crystallized to afford **IVc** (19 mg): mp 52–53.5°C; >95% purity by GC (Table 1); IR, ν_{max} 3300, 3100, 2960–2820, 1740, 1730, 1650, 1550, 1465, 1370, 1260, 1225, 1110, 1095, 1040, 975, 725, 610 cm^{-1} (see also Fig. 4); MS (LKB), *m/z* 365 (3, M−CH_3OH), 338 (17), 281 (4), 278 (7), 262 (5), 253 (100), 170 (7), 144 (10), 123 (10), 109 (25), 102 (32); ^{13}C NMR (25 MHz) data essentially the same as those for **IVc** in Table 2. ^{1}H and ^{13}C NMR analysis of material crystallized after evaporation of fractions 29–32 showed **IIIc, IVc,** and **VII,** in a 1:10:2 ratio. NMR analysis of crystalline material from fractions 33–44 showed **IIIc, IVc,** and **VII** in a 5:2:8 ratio. Data for **IIIc, IVc,** and **VII** obtained from these mixtures are given in Table 1 (TLC and HPLC) and Tables 2, 3, and 4 (^{1}H and ^{13}C NMR).

Compound **Vc.** Fractions 73–148 from column C were evaporated to a residue (74 mg) that was recrystallized twice from hexane to give **Vc** (66 mg): mp 66–67°C; $[\alpha]_D^{27}$ +6.9° (*c* 0.5, chloroform); single component by GC (Table 1); IR, ν_{max} 3300, 3080, 2960–2820, 1740, 1650, 1545, 1465, 1370, 1230, 1140, 1115, 1100, 1085, 1045, 1040, 980, 725, 620, 580 cm^{-1} (see also Fig. 4); MS (ZAB), *m/z* 397 (0.05, M$^+$), 382 (0.2, M−CH_3), 366 (3), 338 (11),

TABLE 4. ^{1}H-^{1}H NMR coupling constants for D-*erythro*- and L-*threo*-sphingosines **I–II**, 3-*O*-methyl ethers **III–IV**, 5-*O*-methyl ethers **V–VI**, and diene **VII**[a–b]

	D-*erythro*- and L-*threo*-Sphingosines						3-*O*-methyl		5-*O*-methyl					Diene
	Ia	**IIa**	*N*-Ac **Ib**	*N*-Ac **IIb**	tri-Ac **Ic**	tri-Ac **IIc**	di-Ac **IIIc**	di-Ac **IVc**[c]	**VIa**	*N*-Ac **Vb**	*N*-Ac **VIb**	di-Ac **Vc**	di-Ac **VIc**	di-Ac **VII**[c]
1a–1b	10.9	10.8	11.3	11.1	11.6	11.4	10.7	11.0	10.4	11.1	11.1	11.3	11.3	11.3
1a–2	6.1	6.3	3.4	4.4	3.9	5.6	3.3	6.9	7.9	5.4	5.4	4.3	4.3	4.5
1b–2	4.6	4.4	3.6	4.2	6.0	5.5	7.2	5.8	4.4	3.8	3.9	5.9	5.9	6.1
2–3	5.5†	5.4†	4.1	3.6	6.0	5.2†[d]	4.5	2.5	6.3	5.6	5.5	5.2	5.1	6.5
2–NH			7.2	7.8	9.3	9.4	8††	8.8		7.6	7.5	8.4	8.3	8.8
3–4	7.2	6.9	6.4	6.6	7.5	7.2†[d]	8.1	8.1	15.5	15.7	15.7	15.7	15.7	15.3
3–5	~1†	1.1	1.3	~1.3	~1†	~0.5†[d]	~1†	~1†	~0.7†	~0.7†	~0.7†			
4–5	15.4	15.4	15.4	15.4	15.3	15.4†[d]	15.3	15.4	7.7	7.3	7.2	7.13	7.29	11.0
5–6a	6.8	6.8	6.8	6.8	6.8	6.8	7.1†	6.7	6.2†	6.4†	6.4†	6.5†	6.4†	10.7
5–6b	6.8	6.8	6.8	6.8	6.8	6.8	7.1†	6.7	6.2†	6.4†	6.4†	6.5†	6.4†	
18–17	7.0	7.0	7.0	7.0	7.0	7.0	7.0†	7.0	7.0	7.0	7.0	7.0	7.0	7.0

[a]Coupling constants in Hz (absolute values) obtained at 500.1 MHz in ~5 mM $CDCl_3$ solution (25°C). Accuracy is ca. ±0.2 Hz except for couplings marked by † (±0.5 Hz). The J_{H4-H5} couplings for **Vc** and **VIc** appear to be accurate to ±0.05 Hz.

[b]Additional couplings observed: all Δ^4 sphingolipids showed J_{H4-H6a} and J_{H4-H6b} of 1.5 Hz; 5-*O*-methyl ethers (**Vb, Vc, VIa, VIb, VIc**) showed J_{H2-H4} of ~1.4 Hz; diene **VII** showed J_{H2-H4} of 1.5 Hz, J_{H5-H7a} of 1.8 Hz, J_{H5-H7b} of 1.8 Hz, J_{H6-H7a} of 7.6 Hz, J_{H6-H7b} of 7.6 Hz, and an unidentified allylic coupling to H-4 of 1.3 Hz. Most allylic couplings were too small to be measured with high accuracy. Additional long-range couplings observed in some spectra could not be reproduced with other samples of the same compound.

[c]Couplings for **IIIc** and **VII** were extracted from spectra of mixtures of **IIIc, IVc,** and **VII** (1:10:2 and 5:2:8).

[d]Couplings roughly estimated from a combination of spin simulation and first-order analysis of multiplet patterns.

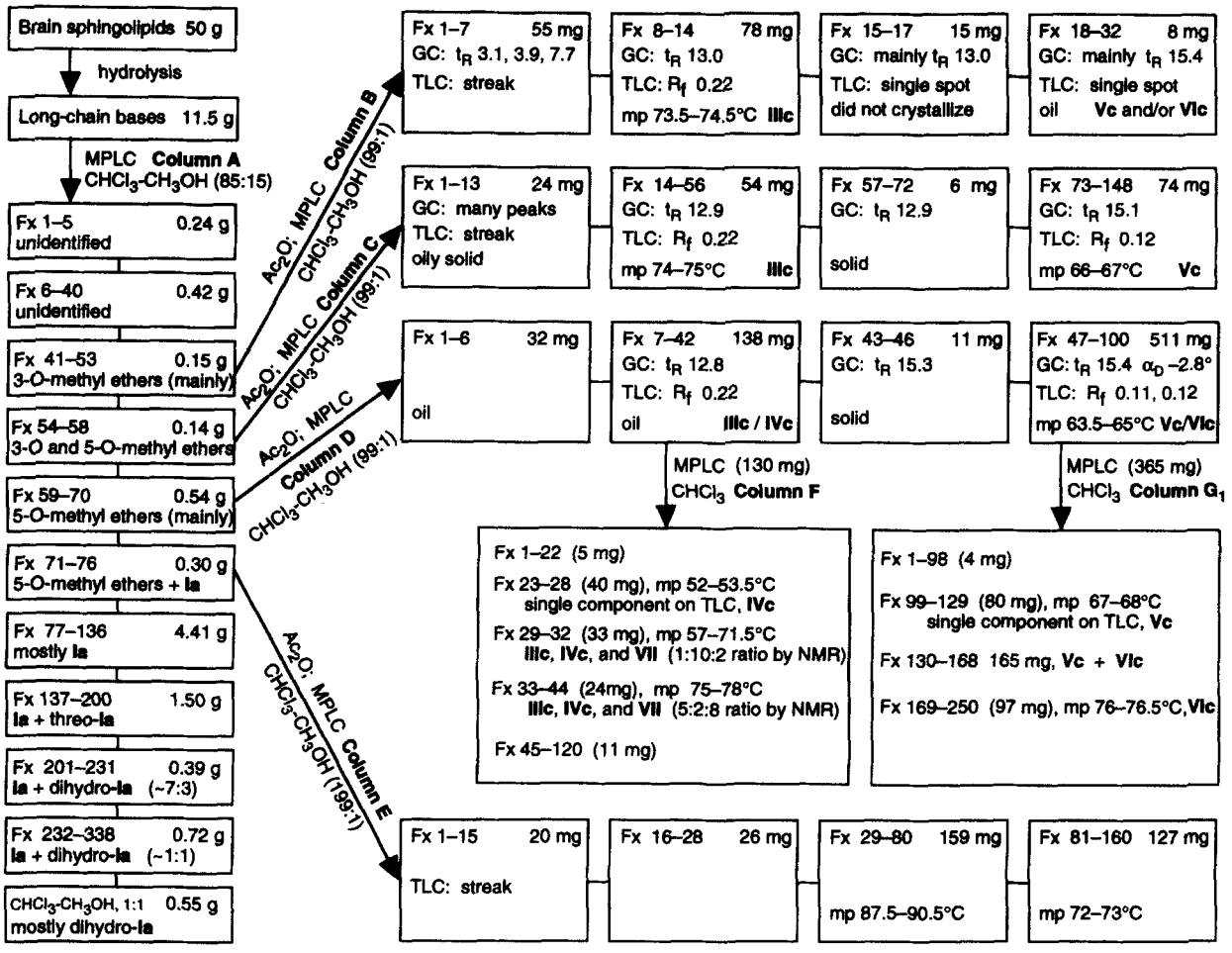

Fig. 3. Summary of MPLC separations of *O*-methyl ether sphingolipids leading to the isolation of **IIIc, IVc, Vc,** and **VIc.** Masses, TLC (SS-1), and GC data (OV-17, 220°C) are given for crude material, whereas melting points are for recrystallized material.

324 (12), 322 (4), 305 (2), 292 (4), 279 (3), 265 (6), 262 (4), 250 (16), 214 (6), 170 (5), 154 (100), 136 (9), 122 (30), 112 (54); ^{1}H NMR showed 98% purity (2% **VIc**); ^{13}C NMR (25 MHz) data essentially the same as those for **Vc** in Table 2. Samples of **Vc** from columns G_1 and G_2 (see below) showed melting points of 67–68°C and 68–69°C, respectively. Additional data for **Vc** are given in Tables 1–4.

Compound ***VIc.*** Fractions 47–100 from column D were evaporated to a solid that was recrystallized from hexane to give a mixture of **Vc** and **VIc** (408 mg): mp 63.5–65°C; $[\alpha]_D^{27}$ −2.8° (chloroform). A portion (365 mg) of this material was subjected to further MPLC (1000 mm × 9 mm silica gel column; elution with chloroform; 6-ml fraction volumes; column G_1). Evaporation of fractions 169–250, followed by recrystallization from hexane gave **VIc** (81 mg): mp 76–76.5°C, $[\alpha]_D^{27}$ −10.3° (*c* 0.5, chloroform); IR, ν_{max} 3300, 3090, 3000–2820, 1740, 1650, 1555, 1470, 1380, 1260, 1115, 1105, 1050, 975, 730, 620 cm^{-1} (see also Fig. 4). A similar MPLC separation (103 mg, column G_2) gave **Vc** (9 mg) and **VIc** (18 mg): mp 75.5–77°C; single component by GC (Table 1). The ^{13}C NMR (25 MHz) data were essentially the same as those for **VIc** in Table 2. Additional data for **VIc** are given in Tables 1–4.

Hydrolysis of the *O*-methyl-sphingosine diacetates to *N*-acetates

A sample of **IIIc** (44 mg; mp 73.5–74.5°C) was hydrolyzed with 0.1 N KOH in water–methanol 1:9 (10 ml) overnight at room temperature. After evaporation of the methanol and addition of water (4 ml), the mixture was extracted with ether (10 ml and 2 × 5 ml). The combined ether extracts were washed with water (2 × 2 ml), and evaporated to dryness. Recrystallization from hexane afforded **IIIb** (9 mg); ^{13}C NMR (25 MHz): δ 169.9, 136.8, 125.7, 84.4, 62.2, 56.8, 53.8, 32.3, 31.9, 29.6, 29.1, 23.4, 22.7, 14.1. Hydrolysis of **Vc** (46 mg; mp 66–67°C) with 0.1 N KOH as described for **IIIc** gave **Vb** (38 mg):

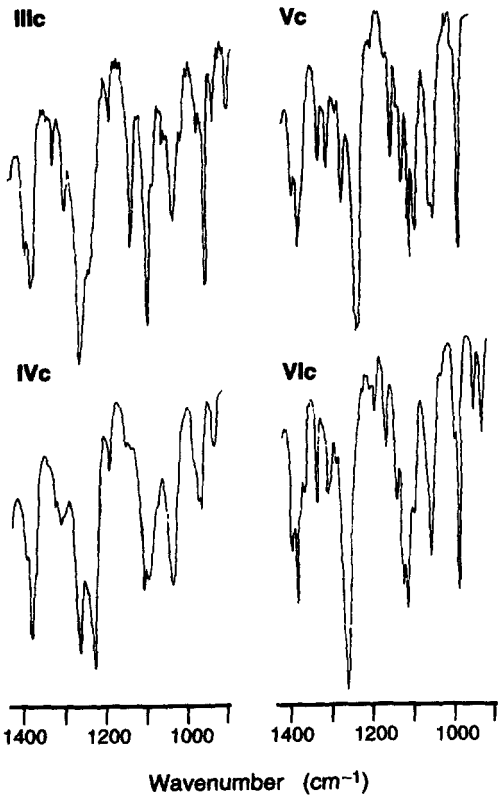

Fig. 4. Fingerprint region of the infrared spectra of *O*-methyl ether diacetates **IIIc, IVc, Vc,** and **VIc.**

mp 73–74°C. Under similar conditions, hydrolysis of **VIc** (51 mg) gave **VIb** (39 mg): mp 77–78.5°C. TLC in SS-4 showed R_f 0.33 for **IIIb** and R_f 0.21 for **Vb,** versus R_f 0.56 for triacetate **Vc.** GC of TMS ethers on OV-17 at 230°C showed the following retention times relative to that of **Ib: IIIb,** 1.08 and **Vb,** 1.26.

Periodate-permanganate oxidation of Ia, IIIc, IVc, Vc, VIa, and VIc

To a solution of sphingolipid base (1–1.5 mg) in *tert*-butanol (0.5 ml), water (0.72 ml), and aqueous K_2CO_3 (0.144 ml, 0.02 M) was added a solution of $NaIO_4$ (6.7 mg) and $KMnO_4$ (0.5 mg) in water (0.31 ml). After 1 h at room temperature, solid $NaHSO_3$ was added, and the resulting colorless solution was treated with 2 N KOH (0.15 ml). After evaporation to dryness under nitrogen, the residue was dissolved in 1 N HCl (0.4 ml) and extracted with ether (2 × 10 ml). The combined ether extracts were washed with water and evaporated to dryness under nitrogen. The resulting residue (in ether–methanol 9:1) was methylated for 30 min with diazomethane solution. After evaporation to dryness, the residue was dissolved in hexane, and analyzed by GC (OV-17; 150°C) and GC–MS. Oxidation products of **Ia, IIIc,** and **IVc** showed a major GC peak at 5.4 min and a minor peak at 3.4 min, whereas oxidation products of **Vc, VIa,** and **VIc** showed peaks at t_R 5.4 min and t_R 19.5 min in a 1:4 ratio. The peaks at t_R 5.4 min from oxidative degradation of **Ia, Vc,** and **VIc** were identified as methyl tetradecanoate by their MS: *m/z* 242 (14, M^+), 211 (8), 199 (14), 185 (4), 157 (4), 143 (17), 129 (6), 101 (7), 87 (63), 74 (100). Formation of methyl tetradecanoate from **Vc** and **VIc** appeared to result from overoxidation (see discussion). The peaks at t_R 19.5 min from oxidative degradation of **Vc,** and **VIc** were identified as methyl 2-methoxypentadecanoate by their MS: *m/z* 286 (1, M^+), 239 (1), 227 (100), 139 (5), 125 (13), 111 (23), 97 (52), 83 (58), 71 (42).

Additional preparation of 5-*O*-methyl ethers (5:1 mixture of VIa:Va)

Beef brain sphingolipids (150 g) prepared as described previously (15) were refluxed for 6 h in methanol (3300 ml) containing 160 ml of conc. H_2SO_4. After extraction of the cooled mixture with petroleum ether, the methanol layer was concentrated to 800 ml and neutralized with 4 N KOH, and precipitated salt was removed by filtration through Celite. The slightly acidic filtrate was made alkaline by addition of 4 N methanolic KOH (25 ml) and extracted with ether. Evaporation of the ether extracts gave a residue (27.6 g) that was chromatographed on silica gel (300 g, 60–200 mesh; elution with chloroform–methanol 97:3; 20-ml fraction volumes). In addition to later-eluting sphingolipids (total 10 g, consisting of **Ia,** its *threo* isomer, and dihydrosphingosine), evaporation of fractions 97–159 gave a residue (5.5 g) that upon recrystallization from ethyl acetate gave an *O*-methyl ether product as colorless crystals (2.7 g): mp, 76–82°C; single component by TLC in SS-5 (R_f 0.66); ≥97% purity by GC (OV-1, 220°C) as the TMS derivative, t_R 8.6 min; $[\alpha]_D^{23}$ −2.9° (*c* 1.2, methanol); ^1H and ^{13}C NMR analysis indicated a 5:1 mixture of **VIa:Va.** Under the same chromatographic conditions, **Ia** showed R_f 0.50 (TLC) and t_R 10.0 min (GC of the TMS derivative). Addition of 2.5% HCl (0.56 ml) in ethanol (10 ml) to the **VIa:Va** mixture (121 mg), followed by evaporation to dryness and recrystallization from ether gave a hydrochloride (95 mg): mp 144–146°C, lit. mp for the hydrochloride of *O*-methylsphingosine II, 143–145°C (19). A mixture of the hydrochloride (370 mg) and 1 N KOH (15 ml) was extracted with ether (60 ml) to give, after recrystallization from ether, the free base: mp 87.5–88°C; $[\alpha]_D^{25}$ −10.4° (*c* 1.2, methanol).

Additional preparation of 5-*O*-methyl ether acetates (mixtures of VIc:Vc and of VIb:Vb)

The diacetate and *N*-acetate derivatives were obtained analogously to the preparation of **Ic** and **Ib** from **Ia.** Thus, acetylation of the 5:1 mixture of **VIa:Va** (1.51 g)

with acetic anhydride-pyridine furnished a crude product (1.57 g) that was purified by MPLC (elution with chloroform–methanol 98:2) to give after recrystallization 5-*O*-methyl ether diacetates (1.33 g): mp 70.5–73°C; single component by TLC in SS-3 (R_f 0.54); IR, ν_{max} 3300, 3090, 3000–2820, 1740, 1645, 1550, 1470, 1380, 1260, 1115, 1100, 1045, 975, 740 cm^{-1}; ^1H and ^{13}C NMR analysis showed a 6:1 mixture of **VIc:Vc.** A portion of the ^1H NMR spectrum is shown in Fig. 2 (panel F).

The 6:1 mixture of **VIc** and **Vc** (1.23 g) was hydrolyzed overnight in 0.1 N methanolic KOH to give a crude product (1.34 g). Recrystallization from hexane afforded colorless crystals (0.90 g): mp 76–77.5°C; single component by TLC in chloroform–methanol 95:5 (R_f 0.13); single component by GC (OV-17; 230°C) as the TMS ether, t_R 14.2 min; IR, ν_{max} 3300, 3100, 3000–2820, 1650, 1580, 1465, 1310, 1135, 1100, 1080, 1070, 1050, 960, 720 cm^{-1}; MS of the TMS ether (LKB), *m/z* 427 (1, M^+), 412 (15), 396 (8), 368 (11), 324 (73), 293 (50), 282 (19), 265 (64), 250 (100), 185 (42), 182 (56), 73 (73); ^1H and ^{13}C NMR analysis showed a 10:1 mixture of **VIb:Vb.**

DISCUSSION

Isolation of *O*-methyl ethers

Under the strongly acidic conditions normally used in sphingolipid hydrolysis, the labile 3-hydroxy-Δ^4 system of sphingosine is prone to allylic rearrangement, dehydration, and epimerization at C-3 (16–18). Until recently (18), the standard solvent for sphingolipid hydrolysis has been methanol (31),[9] which gives rise to an additional set of byproducts, the *O*-methyl ethers. Assuming an S_N1 or S_N1' reaction mechanism with no formation of *cis* isomers and no epimerization at C-2, two 3-*O*-methyl ethers (epimeric at C-3) and two 5-*O*-methyl ethers (epimeric at C-5) can be anticipated.

The first thorough study of *O*-methyl ether byproducts from sphingolipid hydrolysis was done in 1951 by Carter et al. (19), who isolated two substances by repeated recrystallization of 4'-hydroxyazobenzene-4-sulfonate salts. These ethers, designated as *O*-methylsphingosines I and II, were characterized as the free bases, hydrochlorides, *N*-acetates, and diacetates and tentatively identified as 3-*O*-methyl ether epimers.[10] Later studies by Weiss (33) involving oxidative degradation suggested that *O*-methylsphingosines I and II were the 5-*O*-methyl ether epimers, each contaminated with ~30% of 3-*O*-methyl ether. This conclusion was consistent with subsequent observations by GC–MS and HPLC of both 5-*O* and 3-*O*-methyl ethers as byproducts of sphingolipid hydrolysis, with the 5-*O*-methyl ethers usually (34) predominating (31, 34–39). Karlsson (16, 39) reported the isolation of nine C_{18}-sphingosine byproducts, namely the *threo* isomer, four *O*-methyl ether isomers, the two 5-hydroxy-Δ^3 epimers, and two $\Delta^{3,5}$ dienes. Based on Karlsson's samples, the nine byproducts were separated by TLC, as their dinitrophenyl derivatives (34, 40), but further characterization of the samples was apparently never published. The *O*-methyl ethers have been observed in mixtures by TLC, HPLC, GC, and GC–MS (18, 22, 31, 34–39, 41–47), but our analysis of the extensive body of literature on *O*-methyl ethers indicated that the isolation and characterization of individual isomers has never been described, apart from the original publication of Carter et al. (19) on *O*-methylsphingosines I and II.

Our procedure for obtaining the four *O*-methyl ether isomers began with hydrolysis of brain sphingolipids in acidic methanol (1 N HCl, 10 M H_2O), conditions known to give modest quantities of *O*-methyl ethers (31). MPLC of the crude mixture of sphingolipid bases separated D-*erythro*-sphingosine, L-*threo*-sphingosine, and dihydrosphingosine from early fractions consisting mainly of *O*-methyl ethers. Further separation of the *O*-methyl ethers as the free bases appeared unpromising, and subsequent chromatography was done on the diacetates (Fig. 3). Four different fraction sets containing *O*-methyl ethers were acetylated and subjected to MPLC, which afforded a clean separation of the 3-*O*-methyl ethers from the later-eluting 5-*O*-methyl ethers. *O*-Methyl ether epimers **IIIc** and **Vc** predominated in column C (Fig. 3) and were easily isolated by recrystallization. The other *O*-methyl ethers (**IVc** and **VIc**) were initially obtained only as epimeric mixtures (column D), which were resolved by further chromatography (columns F and G_1) with a less polar solvent (chloroform).

In addition to the *O*-methyl ethers, (2R,3E,5Z)-1-acetoxy-2-acetamido-3,5-octadecadiene[6,11] (**VII**) was identified by NMR as the major component of late fractions in the MPLC isolation of **IVc** (Fig. 3, column F). This diene and its 3E,5E isomer have previously been noted as byproducts of sphingolipid hydrolysis (16, 34, 40). We also describe a sphingolipid hydrolysis in nearly anhydrous methanol (1.7 N H_2SO_4, <1 M H_2O) and the

[9]Acid hydrolysis in acetonitrile–water eliminates the formation of *O*-methyl ether byproducts at the expense of increased amounts of *threo*-sphingosines and 5-hydroxy isomers (18, 32). Because O-methyl ether and diene byproducts are readily separated from sphingosine on silica gel, whereas the separation of *erythro* and *threo* isomers is more difficult, aqueous methanolic hydrolysis conditions may be preferred for large-scale preparation of sphingolipid bases.

[10]Work on *O*-methyl ethers is cited with the understanding that 5-*O*-methyl ethers were often erroneously designated as 3-*O*-methyl ethers. The appropriate corrections are apparent from discussions in refs. 33, 35, and 36.

[11]The C-2 configuration is assumed to be unchanged from that in the D-*erythro*-sphingosine. The 2R designation differs from that for natural sphingolipid bases because the change in functionality at C-3 lowers its priority under the RS nomenclature rules.

subsequent chromatographic isolation of a 5:1 mixture of 5-*O*-methyl ethers **VIa** and **Va.** This work, which included the preparation of the diacetate and *N*-acetate derivatives (somewhat more enriched in the 5*S* epimer), illustrated the analysis of such epimeric mixtures by NMR, HPLC, and GC. The results also indicated that epimeric mixtures of 5-*O*-methyl ethers are more readily purified by recrystallization of the hydrochloride than by chromatography or recrystallization of the free base. The ratio of 5-*O*-methyl ether epimers has been reported to vary with sphingolipid hydrolysis conditions (40). This observation is generally compatible with rough estimates of these ratios based upon isolated material derived from our two sphingolipid hydrolyses.

Structure determination

Structures were assigned to the four isomeric *O*-methyl ether diacetates based on their physical, chromatographic, and spectral properties. Two of the *O*-methyl ethers showed distinctive ^{13}C NMR chemical shifts (δ 35.3 and 25.2) indicating a methoxy group at C-5. The other isomers showed NMR data compatible with a methoxy group at C-3. The configuration of the epimeric 3-*O*-methyl ethers was tentatively assigned as indicated in Fig. 1 based upon comparisons of the optical rotation of **IIIc** (−12.1°) with those of the D-*erythro*- and L-*threo*-sphingosine triacetates (−13.8° and +8.4°, respectively) (26), under the assumption that replacement of acetyl by methyl at O-3 has little effect on the rotation. Similar comparisons of NMR data in Tables 2–4 and ^{13}C data for **IIIb** support this inference. The configuration of the 5-*O*-methyl ethers was assigned by correlating their physical and spectral properties with those of *O*-methylsphingosines I and II of Carter et al. (19), for which the C-5 configuration was determined by Weiss (33).[11,12] Olefinic ^{1}H NMR coupling constants of ~15 Hz indicated a *trans* double bond for all the *O*-methyl ether isomers, a finding that had not previously been established unequivocally.

Several original samples of *O*-methylsphingosine I or II (as the free base, *N*-acetate, or diacetate) from the work of Carter et al. (19) were available for the present study. Analysis of these samples by ^{1}H and ^{13}C NMR indicated that *O*-methylsphingosines I and II are the 5-*O*-methyl ether epimers. Correlation of physical and spectral[4] properties (Tables 1–4) showed that the diacetates of *O*-methylsphingosines I and II correspond to **Vc** and **VIc,** respectively. The *O*-methylsphingosine samples showed purities of ~90–99% with little or no contamination by 3-*O*-methyl ethers or the other C-5 epimer. In view of the unavailability of modern chromatographic and spectral methods in 1951, the isolation by Carter et al. (19) of the 5-*O*-methyl ether epimers in quite high chemical purity represented a remarkable achievement.

Weiss (33) concluded that *O*-methylsphingosines I and II of Carter et al. (19) corresponded to 7:3 mixtures of 5-*O*-methyl and 3-*O*-methyl isomers (33). These studies were based on GC analysis of aldehydes obtained by performylation of each *O*-methylsphingosine, followed by hydrolysis and periodate oxidation (**Fig. 5,** scheme B). This conclusion is at variance with the high purity we observed in NMR spectra of the original samples of *O*-methylsphingosines I and II of Carter et al. (19). We have subjected *O*-methyl ethers to periodate–permanganate oxidation (48), followed by methylation and GC–MS analysis (Fig. 5, scheme A). Both **Ia** and 3-*O*-methyl ethers **IIIc** and **IVc** were oxidized to methyl tetradecanoate, whereas 5-*O*-methyl ethers **Vc, VIa,** and **VIc** gave a 4:1 mixture of methyl 2-methoxypentadecanoate and methyl tetradecanoate. Formation of methyl tetradecanoate from the 5-*O*-methyl ethers can be ascribed to overoxidation. As shown in Fig. 5 (scheme B), we propose that Weiss's observation of the tetradecanal degradation product (purportedly arising from 3-*O*-methyl ethers) is attributable to displacement of the methoxyl group (with or without allylic rearrangement) under the acidic performylation conditions or possibly to oxidation of the α-methoxy aldehyde by periodate.

NMR signal assignments

^{1}H and ^{13}C NMR assignments are presented in Tables 2–4 for 3-*O*-methyl ether diacetates, 5-*O*-methyl ethers, their *N*-acetate and triacetate derivatives, D-*erythro*- and L-*threo*-C_{18}-sphingosine, and their *N*-acetate and triacetate derivatives. Special attention was given to the reproducibility of the NMR data in view of the very small chemical shifts differences between *O*-methyl ether epimers. These differences were greatest at polarizable positions, where shieldings are especially susceptible to changes in solvent, temperature, and concentration. Consequently, the NMR spectra were recorded in $CDCl_3$ solution at a standard temperature within a narrow range of concentration. The effects of temperature and concentration on ^{1}H and ^{13}C NMR chemical shifts were measured for several sphingolipid bases. The relationships between chemical shift and temperature were nearly linear in the range of 0°C to 40°C, and the slopes obtained from linear regression for ^{1}H and ^{13}C resonances of representative sphingolipid bases are given in **Table 5.** The relationship between chemical shift and concentration was not expected to be linear, but linear regression over the range of 30–300 mM gave a reasonable fit to the data, allowing the

[12]Weiss (33) determined the C-5 configuration of the 5-*O*-methylsphingosines by comparing the optical rotations of sodium L-2-hydroxypentadecanoate and the enantiomers of sodium 2-methoxypentadecanoate obtained by oxidative degradation of the *O*-methylsphingosines I and II. This assignment of configuration must be regarded as tentative until it is shown that 2-hydroxy and 2-methoxy fatty acid salts have similar rotations in aqueous ethanol.

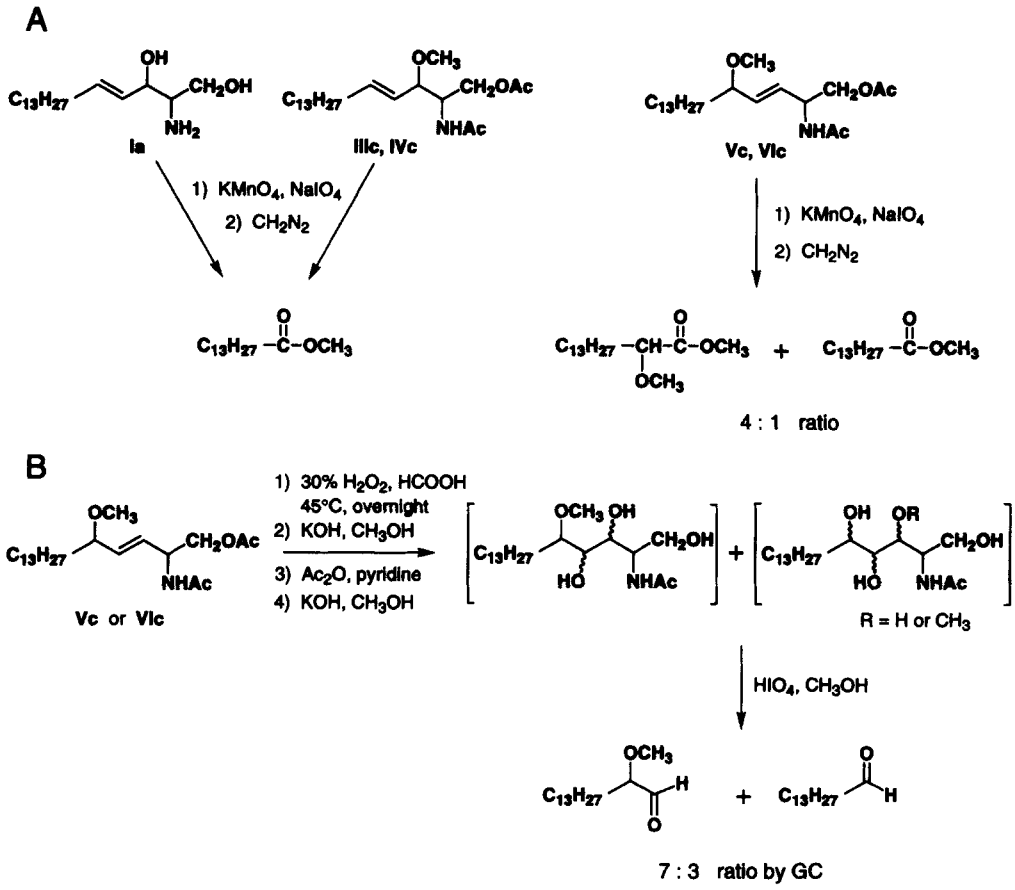

Fig. 5. Oxidative degradation of *O*-methylsphingosines. Scheme A: Periodate-permanganate oxidation of sphingosine and its 3-*O*-methyl and 5-*O*-methyl ethers. Scheme B: Performylation-hydrolysis, followed by periodic acid oxidation reported in ref. 33. We suggest that the minor tetradecanal product may arise from displacement or rearrangement of methoxyl during the acidic conditions of performylation.

concentration effect to be approximated by a single coefficient in this range (Table 5). Thus, although the NMR data presented in Tables 2–4 are strictly valid only for $CDCl_3$ solution at 25°C at the concentrations shown (~5 mM for ^1H, ~60 mM for ^{13}C), compensation for differences in temperature and concentration can be estimated from factors listed in Table 5.

^1H and ^{13}C NMR assignments in Tables 2 and 3 were made from a combination of HSQC, HMBC, double-quantum filtered COSY or COSYDEC, 1-D spectra, and ^1H-^1H coupling patterns. Our assignments appear to be in agreement with those reported previously (49, 50) for sphingolipid bases except for the ^{13}C assignments of C-4 and C-5 of sphingosines **I**–**II**. In an early study of ^{13}C NMR of sphingolipid bases (49), C-4 was reported as the downfield olefinic signal without supporting evidence, and the correctness of this assignment has apparently been accepted by others (26, 50–57). The reported assignments of C-4 and C-5, which have been applied to ceramides and other sphingolipids, seemed to us incompatible with the observation (58, 59) that acetylation of an allylic alcohol leads to shielding of the β-carbon (by 3.6–5.5 ppm) and deshielding of the α-carbon (by 0.1–4.4 ppm). We initially confirmed our suspicions that the reported assignments for C-4 and C-5 were reversed by an early ^1H–^{13}C correlation experiment consisting of a series of single-frequency off-resonance decoupling experiments at different decoupler offsets (60). This experiment showed that the downfield olefinic carbon atom bears the downfield olefinic proton, which is easily assigned as H-5 based on its coupling pattern (doublet of triplets) relative to that of H-4 (doublet of doublets). We have confirmed these findings by an HSQC experiment (Fig. 2, panel A) leading to the same conclusion. HSQC experiments were also used to assign the olefinic ^{13}C signals of the 5-*O*-methyl ethers (Fig. 2, panel B) and of diene **VII.** The structure of **VII** was deduced from HSQC and COSYDEC spectra in conjunction with connectivities obtained by matching ^1H-^1H coupling constants. The *trans-cis* diene system was established from ^1H-^1H NMR coupling constants and confirmed by comparisons with ^1H NMR data for (2E,4Z)-1-acetoxy-2,4-octadiene (61).

TABLE 5. Effect of temperature, concentration, and $Pr(tfc)_3$ on ^1H and ^{13}C NMR chemical shifts of D-*erythro*-sphingosine, *O*-methyl ethers, and their acetate derivatives[a]

	Temperature Coefficients[b]				Concentration Coefficients[c]		Lanthanide-Induced Shifts[d]	
	Ia	**VIa**	**VIb**	**VIc**	**Ia**	**Vb**	**Ia**	**VIa**
C-1	19.6	14.4	7.4	1.5	1.9	−2.1	771	788
C-2	13.3	2.0	8.6	10.2	0.6	−0.4	1000	1000
C-3	12.0	5.1	−3.6	−4.1	0.9	1.2	305	34
C-4	10.4	4.7	17.7	16.5	3.8	−2.1	261	173
C-5	−0.6	1.2	0.5	1.0	2.9	0.0	100	128
C-6	−1.3	4.0	4.7	3.5	0.0	−0.3	70	81
C-7	1.5	0.1	0.3	0.3	0.4	−0.2	51	65
C-8	−1.6	1.4*	1.4*	1.7*	0.1	−0.2	30	41
C-9	−0.7	0.0*	0.3*	0.5*	0.1	−0.2	20	30
C-10	−0.8	0.1	0.1	0.4	0.1	−0.2	14	19
C-11	−0.7	−0.1	0.3**	0.4**	0.1	−0.2	7.9	13
C-12	−0.7	0.0	0.1	0.4	0.1	−0.2	5.1	9.5
C-13	−0.5	−0.1	0.0	0.2	0.2	−0.3	2.8	5.9
C-14	−0.3	−0.1	−0.1**	0.2**	0.2	−0.3	1.3	4.1
C-15	−1.1	−0.9	−0.8	−0.7	0.2	−0.3	0.5	2.4
C-16	0.6	0.6	0.8	0.8	0.2	−0.3	−0.3	1.3
C-17	−0.8	−0.8	−0.4	−0.6	0.2	−0.3	−0.4	0.8
C-18	−4.0	−3.7	−4.0	−3.7	0.3	−0.3	−0.1	0.9
MeO		−0.4	−0.2	0.7		−0.6		75
1-Ac				−4.6				
C=O				−6.7				
2-Ac			−2.5	−3.2		−0.6		
C=O			−8.3	−6.5		0.4		
H-1a	−0.2	−0.3	−0.3	−0.5	−0.2	−0.12		
H-1b	−1.4	−0.7	0.1	0.1	−0.5	−0.23		
H-2	0.5	−1.2	−0.8	−1.0	−1.2	−0.14		
H-3	−0.6	0.0	−0.2	−0.3	−0.9	0.00		
H-4	0.7	0.5	0.7	0.8	−0.1	−0.05		
H-5	0.3	0.1	−0.2	−0.1	−0.3	−0.03		
H-6a		0.2	0.1	−0.1	−0.1	−0.04		
H-6b		0.0	0.0	0.0	−0.1	−0.03		
CH_2[e]	0.4	0.4	0.4	0.4	0.0	0.00		
H-18	0.0	0.0	0.0	0.1	0.0	0.00		
MeO		−0.2	−0.3	−0.2		−0.03		
NH	−24.2	−15.4	−8.1	−4.7	3.8	1.78		
1-Ac				−0.8***				
2-Ac			−1.0	−1.2***		−0.08		

[a]Values marked by asterisks may be interchanged within a column.

[b]In the range of 0–40°C, the effect of temperature on chemical shift was approximated as a linear function described by the equation $\nu = \nu_{25} + k(T - 25)$, where ν_{25} is the chemical shift in ppm at 25°C, T is the temperature in °C, and k is a proportionality constant. The constant k (in units of ppb/°C) was estimated by linear regression from ^1H and ^{13}C NMR spectra recorded in $CDCl_3$ (50–100 mM) at three to five different temperatures in the range of 0°C to 40°C. The accuracy is estimated to be the larger of 10% of the value and ±0.3 ppb/°C (^{13}C) or ±0.1 ppb/°C (^1H). For example, a 10°C increase in temperature will lead to a 0.196 ±0.02 ppm downfield shift for C-1 of **Ia** and an upfield shift of 0.003 ±0.001 ppm for H-1a of **Ia**.

[c]In the range of 30–300 mM, the effect of temperature on chemical shift was approximated as a linear function described by the equation $\nu = \nu_0 + k[S]$, where ν_0 is the chemical shift in ppm at a standard concentration (e.g., 50 mM), [S] is the concentration of sphingolipid base and k is a proportionality constant. The constant k (units of ppb/mM) was estimated by linear regression from ^1H and ^{13}C NMR spectra recorded in $CDCl_3$ at 25°C at three to eight different concentrations in the range 20–270 mM (^{13}C) or 5–270 mM (^1H). The accuracy is rather low, but the coefficients give an idea of the magnitude and direction of the concentration shifts. For example, an increase in concentration from 50 mM to 60 mM will shift the C-1 resonance of **Vb** 0.021 ppm upfield and H-1a of **Vb** 0.001 ppm upfield.

[d]Shifts induced by $Pr(tfc)_3$, normalized to a value of 1000 for the largest induced shift. Positive values correspond to upfield shifts.

[e]Strong "singlet" representing methylene envelope for protons on carbons 8–15.

In previous ^{13}C spectral characterizations of sphingolipid base moieties (20, 26, 49–57), few if any resonances in the nine-carbon cluster of signals at δ 29–30 could be resolved or assigned. As illustrated in Fig. 2 (panels C and D), nearly all of the ^{13}C signals were isolated by resolution enhancement of the 126-MHz spectra. The signals were assigned by LIS experiments, in which the $Pr(tfc)_3$-induced shifts[13] of each carbon atom were measured precisely. The LIS values, shown in Table 5, indicated that $Pr(tfc)_3$ coordinated almost exclusively to functional groups at C-1 and C-2. LIS results are normally interpreted using the simplified McConnell-Robertson equation (62), where k is a proportionality constant and r and θ are defined in Fig. 5.

$$LIS_{calculated} = k(3\cos^2\theta - 1)/r^3$$

Although multiple sites of coordination and multiple conformations of the sphingolipid bases precluded exact predictions of LIS, this equation did lead to the useful inference that both θ and r increase with increasing carbon number when the sphingolipid base is in the representative fully extended conformation (**Fig. 6**). Under the reasonable assumption that $\theta < 90°$, the equation then predicts a decrease[5] in LIS with increasing carbon number.

This predictive model was validated by the observation of decreasing LIS for carbons 4–7, for which independent assignments were available. The remaining carbons were assigned to give a pattern of decreasing LIS with increasing carbon number. The point in the sphingolipid chain at which LIS values became too small for reliable assignments (C-16) was the point at which assignments had already been determined by other methods. The LIS-derived assignments for sphingosine (**Ia**) and *O*-methylsphingosine II (**VIa**) were mutually compatible in that chemical shifts were nearly identical between **Ia** and **VIa** for carbons 10–14, whereas carbons 7–9 showed small deviations attributable to differences in functionality at C-5. Carbons 7–15 of other sphingolipid bases in Table 2 (except **VII**) were easily assigned by chemical shift comparisons with **Ia** or **VIa.** These findings, which are consistent with ^{13}C data for methyl stearate (63), represent the first complete ^{13}C NMR assignments for sphingolipid bases. These assignments may be of value in structure determinations and in studies relating nuclear Overhauser enhancements and T_1 values of individual carbon atoms to the rotational dynamics of the sphingolipid chain.

[13]A praseodymium shift reagent was chosen for its upfield induced shifts, which were expected to promote dispersion of the cluster of ^{13}C signals at δ 29–30. The subsequently observed pattern for carbons 7–13 of increasing ^{13}C chemical shift with increasing carbon number indicated that a europium or ytterbium reagent would have shifted the signals into each other, resulting in several confusing crossovers.

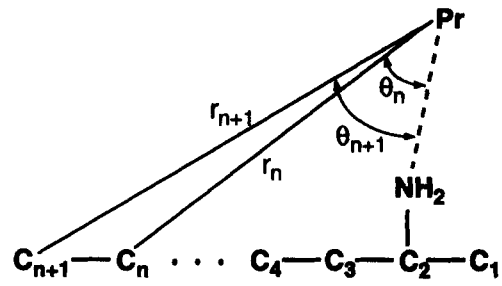

Fig. 6. Idealized picture of the praseodymium atom of $Pr(tfc)_3$ binding to a sphingolipid base at the C-2 nitrogen; C_n is the n^{th} carbon atom in the sphingolipid chain, r_n is the distance between the Pr atom and the substrate atom C_n, and θ_n is the angle between Pr—C_n and the principal magnetic axis (e.g., Pr—N). Analogous definitions hold for C_{n+1}, r_{n+1}, and θ_{n+1}. This diagram illustrates how both θ and r increase with increasing n.

Methods for identifying *O*-methyl ether isomers

The ^{13}C NMR data in Table 2 were useful in determining the composition of sphingolipid base mixtures containing *O*-methyl ethers. *O*-Methyl ethers were readily distinguished from other sphingosine derivatives by the distinctive ^{13}C NMR chemical shift ($\delta \sim 80$) of the carbon atom bearing methoxyl. The 5-*O*-methyl ethers were recognized by the C-6 (δ 35.3) and C-7 (δ 25.2) resonances, which were well-separated from the corresponding signals in 3-*O*-methyl ethers (δ 32.3 and δ 29.1) and most other sphingolipid bases. The 3-*O*-methyl ether epimers could be distinguished from each other by their C-3 chemical shifts (δ 82.4 vs. δ 80.0 for the diacetate derivatives), but the ^{13}C NMR spectra of the 5-*O*-methyl epimers were very similar, especially for the free bases **Va** and **VIa.** Identification of a single 5-*O*-methyl ether epimer from its ^{13}C spectrum requires reproducibility of ± 0.01 ppm, which might be achieved (except for C-2 and the olefinic carbons) by exclusion of polar impurities and careful attention to temperature and concentration. Solvent, temperature, and concentration had a somewhat smaller effect on ^1H chemical shifts, which were also useful for analyzing *O*-methyl ether mixtures. As in the case of ^{13}C spectra, the 3-*O*-methyl ether diacetates are easily distinguished (e.g., by the separation of the H-1 resonances), whereas differentiation of the 5-*O*-methyl ethers requires careful chemical shift comparisons, with special attention to operating conditions if only one isomer is available. The relative ease of differentiating *O*-methyl ether epimers by ^1H NMR at 500 MHz is illustrated in Fig. 2, in which the reasonably well-dispersed signals in mixtures of 3-*O*-methyl ethers **IIIc** and **IVc** (panel E) are contrasted with the largely unresolved signal pairs of the 5-*O*-methyl ether diacetates **Vc** and **VIc** (panel F). Diacetates **Vc** and **VIc** also showed differences in the J_{H4-H5} coupling constant large enough to be used in their identification.

As shown in Fig. 4, the *O*-methyl ether diacetates could also be distinguished from the fingerprint region of the IR spectrum. This region, which contains the strong bands corresponding to C—O and C—O—C stretching vibrations, differed markedly among the four isomers **IIIc, IVc, Vc,** and **VIc.** Mass spectra of the 3-*O*-methyl ether diacetates also differed from those of the 5-*O*-methyl isomers, as has been reported previously for other derivatives (38).

Chromatographic data for the *O*-methyl ethers are summarized in Table 1. The 3-*O*-methyl ethers were well-separated from the 5-*O*-methyl ethers by TLC, HPLC, and GC as the diacetates, with retention orders paralleling those given previously for TLC (34, 35, 40), GC (17, 31), and HPLC (18, 37, 38) despite differences in derivatization and operating conditions. Apart from TLC of dinitrophenyl derivatives (34, 40), chromatographic separations of epimeric pairs of *O*-methyl ethers have not been reported. We observed partial separation of epimeric pairs of *O*-methyl ether diacetates by reversed phase HPLC (**Fig. 7**), but the resolution was insufficient for quantitation of minor epimeric components. The *N*-acetates of the 5-*O*-methyl ethers were not resolved under the conditions in Fig. 7, but were partially resolved in a weaker solvent. Other derivatizations or chromatographic techniques (e.g., capillary GC or normal phase HPLC) may be needed to adequately resolve these highly similar pairs of epimers. Because triacetate **Ic** and the *O*-methyl ether diacetates showed similar chromatographic behavior on TLC and reversed phase HPLC, sphingosine samples cannot be analyzed for *O*-methyl ether impurities by liquid chromatography of the triacetate derivatives.

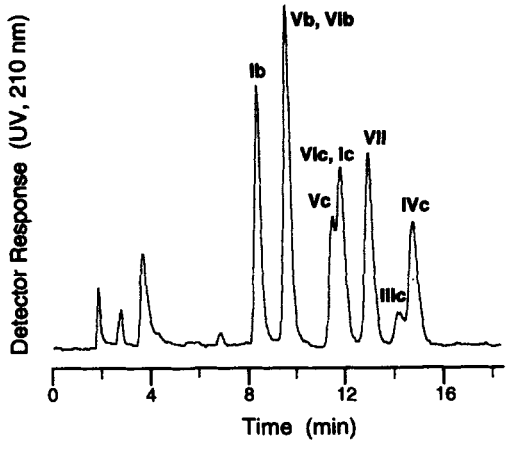

Fig. 7. Reversed phase HPLC separation of 3-*O*-methyl and 5-*O*-methyl ether diacetates (water–methanol 1:9). The chromatogram was obtained by injecting a mixture of **Ib, Vb, Ic, IIIc, Vc, VIc,** and fractions 29–32 of column F. Peak labels for **VIb** and **Ic** correspond to the retention times of these compounds in other chromatograms, in which they were not resolved from **Vb** and **VIc,** respectively.

In summary, we have isolated as diacetates the four *O*-methyl ether byproducts formed during methanolic hydrolysis of sphingolipids. The 3-*O*-methyl ethers were easily differentiated from the 5-*O*-methyl ethers by TLC, HPLC, GC, MS, IR, and ^{1}H and ^{13}C NMR, but epimeric ethers were difficult to distinguish and quantify in mixtures except by NMR, which required careful attention to operating conditions in the case of the highly similar 5-*O*-methyl ethers. The diacetates of *O*-methylsphingosines I and II of Carter et al. (19) were correlated with the 5-*O*-methyl ether epimers according to physical and spectral properties. This correlation together with an earlier structure determination by Weiss (33) was used to assign tentatively the C-5 configuration of the 5-*O*-methyl ether epimers, and the C-3 configuration of the 3-*O*-methyl ethers was assigned tentatively from correlations of optical rotations. The chromatographic and ^{1}H and ^{13}C NMR spectral properties of each of the four *O*-methyl compounds presented herein should be valuable for the characterization of sphingosine samples and evaluation of their purity. In addition, the availability of the individual epimers should permit their use in structure–activity relationships with regard to effect of sphingolipid bases (and their derivatives) on various biological phenomena reported to be affected by sphingosine and its 1-phosphate[14] and *N*-acyl derivatives.

This work was supported in part by the Ralph and Dorothy Looney Endowment Fund and grants from the National Institutes of Health (HL-15376 and HL-49122) and the Robert A. Welch Foundation (C-583). We thank the Shell Development Company for the generous gift of a ZAB-HF mass spectrometer. The Rice University 500 MHz NMR Facility was established with the support of NIH grant RR05759 and the W. M. Keck Foundation.

Manuscript received 19 August 1994 and in revised form 22 November 1994.

REFERENCES

1. Dyatlovitskaya, E. V., and L. D. Bergelson. 1987. Glycosphingolipids and antitumor immunity. *Biochim. Biophys. Acta.* **907:** 125–143.
2. Fishman, P. H. 1982. Role of membrane gangliosides in the binding and action of bacterial toxins. *J. Membrane Biol.* **69:** 85–97.
3. Karlsson, K-A. 1989. Animal glycosphingolipids as membrane attachment sites for bacteria. *Annu. Rev. Biochem.* **58:** 309–350.
4. Schwarzmann, G., and K. Sandhoff. 1990. Metabolism and intracellular transport of glycosphingolipids. *Biochemistry.* **29:** 10865–10871.

[14]It should be noted that the 1-phosphate derivative of 5-methoxydihydrosphingosine was prepared by Weiss (64) from *O*-methylsphingosine II of Carter et al. (19).

5. Hakomori, S. 1981. Glycosphingolipids in cellular interaction, differentiation, and oncogenesis. *Annu. Rev. Biochem.* **50:** 733–748.
6. Hakomori, S. 1990. Bifunctional role of glycosphingolipids. Modulators for transmembrane signalling and mediators for cellular interactions. *J. Biol. Chem.* **265:** 18713–18716.
7. Sandhoff, K. 1977. The biochemistry of sphingolipid storage diseases. *Angew. Chem. Int. Ed. Engl.* **16:** 273–283.
8. Pentcher, P. G., and J. A. Barranger. 1978. Sphingolipidoses: molecular manifestations and biochemical strategies. *J. Lipid Res.* **19:** 401–409.
9. Hanada, K., M. Nishijima, M. Kiso, and Y. Akamatsu. 1992. Sphingolipids are essential for growth of Chinese hamster ovary cells: restoration of growth of a mutant defective in sphingolipid base biosynthesis by exogenous sphingolipids. *J. Biol. Chem.* **267:** 23527–23533.
10. Hannum, Y. A., and R. M. Bell. 1989. Functions of sphingolipids and sphingolipid breakdown products in cellular recognition. *Science.* **243:** 500–507.
11. Merrill, A. H., Jr. 1991. Cell regulation by sphingosine and more complex sphingolipids. *J. Bioenerg. Biomembr.* **23:** 83–104.
12. Hannum, Y. A. 1994. The sphingomyelin cycle and the second messenger function of ceramide. *J. Biol. Chem.* **269:** 3125–3128.
13. Kolesnick, R., and D. W. Golde. 1994. The sphingomyelin pathway in tumor necrosis factor and interleukin-1 signalling. *Cell.* **77:** 325–328.
14. Su, Y., D. Rosenthal, M. Smulson, and S. Spiegel. 1994. Sphingosine-1-phosphate, a novel signalling molecule stimulates DNA binding activity of AP-1 in quiescent Swiss 3T3 fibroblasts. *J. Biol. Chem.* **269:** 16512–16517.
15. Carter, H. E., W. J. Haines, W. E. Ledyard, and W. P. Norris. 1947. Biochemistry of the sphingolipides. Preparation of sphingolipides from beef brain and spinal cord. *J. Biol. Chem.* **169:** 77–82.
16. Karlsson, K-A. 1970. On the chemistry and occurrence of sphingolipid long-chain bases. *Chem. Phys. Lipids.* **5:** 6–43.
17. Karlsson, K-A. 1970. Sphingolipid long chain bases. *Lipids.* **5:** 878–891.
18. Kadowaki, H., E. G. Bremer, J. E. Evans, F. B. Jungalwala, and R. H. McCluer. 1983. Acetonitrile-hydrochloric acid hydrolysis of gangliosides for high performance liquid chromatographic analysis of their long chain bases. *J. Lipid Res.* **24:** 1389–1396.
19. Carter, H. E., O. Nalbandov, and P. A. Tavormina. 1951. Biochemistry of the sphingolipides. The O-methyl ethers of sphingosine. *J. Biol. Chem.* **192:** 197–207.
20. Pinkerton, F. D., A. Kisic, W. K. Wilson, and G. J. Schroepfer, Jr. 1993. D-*Erythro*-sphingosine lowers 3-hydroxy-3-methylglutaryl coenzyme A reductase activity in Chinese hamster ovary cells. *Biochem. Biophys. Res. Commun.* **190:** 63–69.
21. Bodenhausen, G., and D. J. Ruben. 1980. Natural abundance nitrogen-15 NMR by enhanced heteronuclear spectroscopy. *Chem. Phys. Lett.* **69:** 185–189.
22. Carter, H. E., and R. C. Gaver. 1967. Improved reagent for trimethylsilylation of sphingolipid bases. *J. Lipid Res.* **8:** 391–395.
23. Kulmacz, R. J., A. Kisic, and G. J. Schroepfer, Jr. 1979. Sphingolipid base metabolism. Chemical syntheses and properties of *N*-acetyl derivatives of 4R-, 4S-, 5R-, and 5S-hydroxysphinganine. *Chem. Phys. Lipids.* **23:** 291–319.
24. Shapiro, D., H. Segal, and H. M. Flowers. 1958. The total synthesis of sphingosine. *J. Am. Chem. Soc.* **80:** 1194–1197.
25. Gaver, R. C., and C. C. Sweeley. 1966. Chemistry and metabolism of sphingolipids. 3-Oxo derivatives of *N*-acetylsphingosine and *N*-acetyldihydrosphingosine. *J. Am. Chem. Soc.* **88:** 3643–3647.
26. Tkaczuk, P., and E. R. Thornton. 1981. Useful syntheses of *erythro*- and *threo*-*N*-oleoyl-D-sphingosines (ceramides) and galactosylceramides (cerebrosides) from L-serine. *J. Org. Chem.* **46:** 4393–4398.
27. Garner, P., J. M. Park, and E. Malecki. 1988. A stereodivergent synthesis of D-*erythro*-sphingosine and D-*threo*-sphingosine from L-serine. *J. Org. Chem.* **53:** 4395–4398.
28. Garigipati, R. S., A. J. Freyer, R. R. Whittle, and S. M. Weinreb. 1984. Diastereoselective synthesis of unsaturated vicinal amino alcohols via Diels-Alder reactions of *N*-sulfinyl dienophiles. *J. Am. Chem. Soc.* **106:** 7861–7867.
29. Grob, C. A., and F. Gadient. 1957. Die Synthese des Sphingosins und seiner Stereoisomeren. *Helv. Chim. Acta.* **40:** 1145–1157.
30. Polt, R., M. A. Peterson, and L. DeYoung. 1992. Aluminoxy acetals from α-amino esters: chirality transfer via sequential addition of hydride and C-nucleophiles. 2-Amino alcohols and sphingosines. *J. Org. Chem.* **57:** 5469–5480.
31. Gaver, R. C., and C. C. Sweeley. 1965. Methods for methanolysis of sphingolipids and direct determination of long-chain bases by gas chromatography. *J. Am. Oil Chem. Soc.* **42:** 294–298.
32. Nishimura, K., and A. Nakamura. 1985. High performance liquid chromatographic analysis of long chain bases in intestinal glycolipids of adult and embryonic Japanese quails. *J. Biochem.* **98:** 1247–1254.
33. Weiss, B. 1964. Partial identity of sphingosine methyl ethers. *Biochemistry.* **3:** 1288–1293.
34. Michalec, Č., and Z. Kolman. 1968. Biochemistry of sphingolipids. Identification of sphingosine base degradation products originating from different acid hydrolytic conditions. *J. Chromatogr.* **34:** 375–381.
35. Taketomi, I., and N. Kawamura. 1972. Degradation of sphingosine bases during acid hydrolysis of sphingomyelin, cerebroside or psychosine. *J. Biochem.* **72:** 189–193.
36. Polito, A. J., T. Akita, and C. C. Sweeley. 1968. Gas chromatography and mass spectrometry of sphingolipid bases. Characterization of sphinga-4,14-dienine from plasma sphingomyelin. *Biochemistry.* **7:** 2609–2614.
37. Jungalwala, F. B., J. E. Evans, H. Kadowaki, and R. H. McCluer. 1984. High performance liquid chromatography–chemical ionization mass spectrometry of sphingoid bases using moving-belt interface. *J. Lipid Res.* **25:** 209–216.
38. Jungalwala, F. B., J. E. Evans, E. Bremer, and R. H. McCluer. 1983. Analysis of sphingoid bases by reversed-phase high performance liquid chromatography. *J. Lipid Res.* **24:** 1380–1388.
39. Karlsson, K. A. 1963. Studies on sphingosines. The isolation and preliminary identification of some preparative byproducts of C18 sphingosine. *Acta. Chem. Scand.* **17:** 903.
40. Michalec, C., J. Ledvinová-Reinišová, and Z. Kolman. 1980. Biochemistry of sphingolipids. Thin-layer microchromatography of DNP derivatives of long-chain bases on Silufol$_{UV\ 254}$ sheets. *J. Chromatogr.* **190:** 498–500.
41. Sambasivarao, K., and R. H. McCluer. 1963. Thin-layer chromatographic separation of sphingosine and related bases. *J. Lipid Res.* **4:** 106–108.
42. Karlsson, K-A. 1965. Studies on sphingosines. Use of trimethylsilyl ethers for the gas chromatography and mass spectrometry of sphingosines. *Acta. Chem. Scand.* **19:** 2425–2427.
43. Akino, T. 1968. Studies on sphingolipids. Gas-liquid chro-

matographic analyses of sphingosine bases. *Sapporo Med. J.* **34:** 255–265.
44. Gilliland, K. M., and E. A. Moscatelli. 1969. Sphingolipids of animal nervous tissue. A comparative study of polar lipid sphingosine bases. *Biochim. Biophys. Acta.* **187:** 221–229.
45. Moscatelli, E. A., and E. Isaacson. 1969. Gas–liquid chromatographic analysis of sphingosine bases in sphingolipids of human normal and multiple sclerosis cerebral white matter. *Lipids.* **4:** 550–555.
46. Taketomi, T., and N. Kawamura. 1970. Preparation of lysohematoside (neuraminyl-galactosyl-glucosylsphingosine) from hematoside of equine erythrocyte and its chemical and hemolytic properties. *J. Biochem.* **68:** 475–485.
47. Isaacson, E., and E. A. Moscatelli. 1970. Sphingolipids of developing human central nervous tissue: changes in composition of sphingosine bases. *J. Neurochem.* **17:** 365–371.
48. Scheuerbrandt, G., and K. Bloch. 1962. Unsaturated fatty acids in microorganisms. *J. Biol. Chem.* **237:** 2064–2068.
49. Stoffel, W., O. Zierenberg, and B. D. Tunggal. 1972. ^{13}C-nuclear magnetic resonance spectroscopic studies on saturated, mono-, di- and polyunsaturated fatty acids, phospho- and sphingolipids. *Hoppe Seylers Z. Physiol. Chem.* **354:** 1962–1969.
50. Bruzik, K. S. 1988. Synthesis and spectral properties of chemically and stereochemically homogenous sphingomyelin and its analogues. *J. Chem. Soc. Perkin Trans. 1:* 423–431.
51. Sarmientos, F., G. Schwarzmann, and K. Sandhoff. 1985. Direct evidence by carbon-13 NMR spectroscopy for the *erythro* configuration of the sphingoid moiety in Gaucher cerebroside and other natural sphingolipids. *Eur. J. Biochem.* **146:** 59–64.
52. Sripada, P. K., P. R. Maulik, J. A. Hamilton, and G. G. Shipley. 1987. Partial synthesis and properties of a series of *N*-acyl sphingomyelins. *J. Lipid Res.* **28:** 710–718.
53. Hara, A., and T. Taketomi. 1986. Chemical properties and stereoisomerism of heterogeneous long chain bases in lysosphingolipids by positive ion fast atom bombardment mass spectrometry and carbon-13 NMR spectroscopy. *J. Biochem.* **100:** 415–423.
54. Ahmad, T. Y., J. T. Sparrow, and J. D. Morrisett. 1985. Fluorine-, pyrene-, and nitroxide-labeled sphingomyelin: semi-synthesis and thermotropic properties. *J. Lipid Res.* **26:** 1160–1165.
55. Koerner, T. A. W., Jr., L. W. Cary, S-C. Li, and Y-T. Li. 1979. Carbon 13 NMR spectroscopy of a cerebroside. — *J. Biol. Chem.* **254:** 2326–2328.
56. Harris, P. L., and E. R. Thornton. 1978. Carbon-13 and proton nuclear magnetic resonance studies of gangliosides. *J. Am. Chem. Soc.* **100:** 6738–6745.
57. Sillerud, L. O., R. K. Yu, and D. E. Schafer. 1982. Assignment of the carbon-13 nuclear magnetic resonance spectra of gangliosides G_{M4}, G_{M3}, G_{M1}, G_{D1a}, G_{D1b}, and G_{T1b}. *Biochemistry.* **21:** 1260–1271.
58. Wenkert, E., M. J. Gasic, E. W. Hagaman, and L. D. Kwart. 1975. Long range substituent effects reflected in the ^{13}C NMR spectra of allyl alcohols and their derivatives. *Org. Magn. Reson.* **7:** 51–53.
59. Tsuda, M., E. J. Parish, and G. J. Schroepfer, Jr. 1979. Carbon-13 nuclear magnetic resonance studies of allylic hydroxysterols. Assignment of structure to 5α-cholest-8(14)-ene-3β,7α,15α-triol, an inhibitor of sterol synthesis. *J. Org. Chem.* **44:** 1282–1289.
60. Wehrli, F. W., A. P. Marchand, and S. Wehrli. 1988. Interpretation of Carbon-13 NMR Spectra. 2nd Ed. John Wiley & Sons, New York, NY. 101–114.
61. Commerçon, A., J. F. Normant, and J. Villieras. 1980. Substitution des halogéno-1 alcynes-1 par les dérivés organométalliques du cuivre. Accès à une nouvelle classe de synthons: application à la synthèse du bombykol. *Tetrahedron.* **36:** 1215–1221.
62. Wenzel, T. 1987. NMR Shift Reagents. CRC Press, Boca Raton, FL. 169–183.
63. Gunstone, F. D. 1992. High-resolution ^{1}H and ^{13}C NMR. *In* Lipid Analysis. A Practical Approach. R. J. Hamilton and S. Hamilton, editors. Oxford University Press, Oxford, UK. 243–262.
64. Weiss, B. 1957. Synthesis of several phosphorylated derivatives of dihydrosphingosine. *J. Am. Chem. Soc.* **79:** 5553–5557.